

EXPERIMENTAL RESEARCH AND MODELING OF NORMAL CONTACT STIFFNESS AND CONTACT DAMPING OF MACHINED JOINT SURFACES

Konrad Konowski

Summary

The present paper presents a test stand used to measure normal contact stiffness of flat contact joints of steel surfaces subjected to mechanical treatment. The test stand was used to determine the dependence of normal contact displacements on contact pressures. On the basis of the obtained characteristics a non-linear model of a contact joint was developed. The model describes a dependence of normal contact stiffness and damping on mean pressures and the amplitude of dynamic load with a harmonic course. The model was based on the Kelvin-Voight model widely used in the literature on the subject taking into consideration the stiffness and damping variable.

Keywords: contact stiffness, damping, experimental research, hysteresis loops

Badania doświadczalne oraz modelowanie sztywności stykowej normalnej i tłumienia w połączeniach elementów maszyn

Streszczenie

W pracy przedstawiono stanowisko do badania stykowej sztywności normalnej płaskich połączeń stykowych i powierzchni elementów stalowych po obróbce mechanicznej. Wyznaczono zależność odkształcenia stykowego normalnego od nacisku powierzchniowego. Na podstawie uzyskanych charakterystyk opracowano model nieliniowy połączenia stykowego, który opisuje zależność sztywności stykowej normalnej i tłumienia od średnich wartości nacisku oraz amplitudy obciążenia dynamicznego o przebiegu harmonicznym. Podstawą opracowania jest model ciała lepko-sprężystego Kelvina-Voighta, przy uwzględnieniu zmiennej sztywności i tłumienia.

Słowa kluczowe: sztywność stykowa, tłumienie, badania doświadczalne, pętle histerezy

1. Introduction

Machines and mechanical devices are usually made up of many elements and assemblies connected with one another either immovable manner (bolted joints, shrink fit joints) or movable manner (slideways, bearings). These joints are essential to assure smooth running operation of machines, particularly when they are subjected to dynamic load. Owing to this fact the issue of joints has

Address: Konrad KONOWALSKI, Ph.D. Eng., Faculty of Mechanical Engineering and Mechatronics Szczecin University of Technology, 70-300 Szczecin, Poland, e-mail:konrad.konowski@ps.pl

been often analyzed in various experimental research projects as well as widely discussed in theoretical papers [1-9]. Correct modeling of machine elements and their connections increases the precision of calculations and makes it possible to conduct a computer simulation of their behavior as early as at the design stage. Methods of how to calculate and rationally shape individual machine elements taking into consideration their strength (especially volumetric strength) and stiffness have been well developed and these methods have been for years used in designing machines (e.g. FEM). The state-of-the-art knowledge about constructional connections and methods of how to calculate them is quite inadequate in the face of current and fast growing needs in this field. Many experiments and day-to-day practice have demonstrated [2-7] that they are not elements themselves, but their connections that are the weakest link in the structure of mechanical systems of many machines. Therefore, there is a need to develop reliable models of such connections. In phenomenological approach modeling of contact joints is conducted on the basis of their static and dynamic characteristics. In every day practice, very simplified linear models which describe various contact phenomena are used for the necessary calculations. And this is true even though there are a number of experimental papers tackling the issue. This kind of simplification makes it impossible to properly understand physical phenomena taking place in contact joints. Needless to say, this can also lead to gross errors. This is particularly true of contact joints which are weakly loaded with normal forces, including joints of machines, production systems, measuring devices, etc. For practical calculations, FEM commercial codes such as ADINA [10], ANSYS [11], ABAQUS are usually used. The systems most often also contain procedures used to analyze contact phenomena. Two basic algorithms and their modifications are widely used [12]. The first algorithm is the Lagrange Multiplier Method and the other the Penalty Function Method. Both algorithms solve two basic problems, the first of which is how to determine the volume and amount of the surface area, lines and points coming into contact. These parameters often change when a system undergoes dynamic load changes. Owing to the fact that boundary conditions can undergo various changes, a contact phenomena should be treated as a non-linear phenomena. The other problem concerns determining mutual influences of surfaces, lines or points coming into contact. This requires selecting reliable models of contact joints and choosing their parameters. One of the basic parameters chosen by a system's user is contact stiffness. If this stiffness is too high, problems arise in reaching solution convergence or else we obtain matrix singularity of a system of equations. If the stiffness is too low, the solution may turn out to be imprecise or singular. These are typical problems any user of FEM has to face and overcome by means of a trial and error approach. In order to make calculations easier, some FEM models include procedures which automatically adopt stiffness of these elements making it possible to both achieve convergence and to maintain the necessary precision of their solutions. However, characteristics of contact

stiffness used in these calculations are often quite different from those which are experimentally determined.

Bearing in mind these facts, it is necessary to continue further experimental research into contact joints. It is also evident that new, more precise and non-linear models should be developed for contact joints. These models are necessary to properly understand current problems of compound systems dynamics and to be able to solve these problems using computer simulation methods. This paper aims at developing and analyzing such a model that could be used in the field of machines' dynamics.

2. Experimental research of flat contact joints loaded with normal forces

The experiments were performed on a test stand that was constructed specially for these purposes [7]. A diagram of the test stand is shown in Fig. 1. A typical feature of experimental research into contact joints is that even relatively high load results in a very small contact displacement, which amounts to anything between a few and several dozen micrometers, while their runs in the load function are non-linear. Contact displacement happening as a result of cyclically applied dynamic load given a stable working load amounts to 1 μm , or can even be smaller.

A pair of samples which actually made up the investigated contact joint (Fig. 1) was placed on a plate 4, in a stiff frame. The samples were shaped as cylinders with centrally located holes. They were made of steel C45, hardness 45-55 HRC. The investigated contact were the end faces of the samples, which

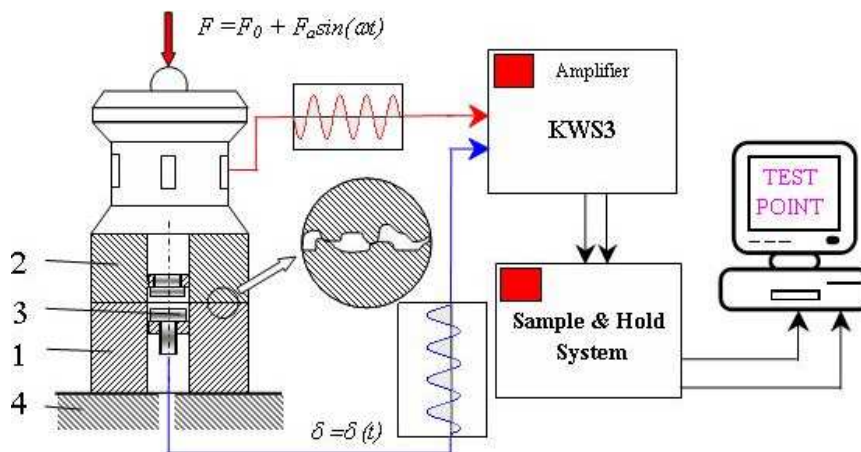


Fig. 1. A diagram of the test stand used to investigate normal contact stiffness and damping

were pressed to each other with a force $F(t)$. The contact surface of the samples had a shape of a flat ring and the nominal area of the surface was $A = 50 \text{ cm}^2$. Average surface pressure p was calculated as the ratio of force $F(t)$ to the nominal area of the contact surface A .

The contact surfaces of samples 1 and 2 had been ground. Their parameters and their geometrical structure were measured. These measurements were performed on a computerized station designed to measure geometrical state of surfaces and contours (SUPSGPiK) manufactured by Hommelwerke T8000. Ten measurements were made for each ground surface. The obtained mean values of the measured parameters are presented in Table 1.

Table 1. The parameters of roughness of the specimens

Parameter	Displacements, μm	
	Specimen 1	Specimen 2
R_{max}	2.27	2.57
R_a	0.26	0.37
R_q	0.33	0.46

The traces of surface treatment were placed perpendicularly. The samples were subjected to (static and dynamic) load by means of a controlled, hydraulic system.

The tests were carried out in the range of constant pressure of $p_o = 0,5-2,5$ MPa with harmonic runs with the amplitude of $p_a = 0,4$ MPa. The total number of load cycles in each trial was 1500. Then it was assumed that the normal characteristics were stabilized.

After having loaded the contact interface up to the value of contact pressure p_o (constant load), it was assumed that it was the zero level of dynamic pressure. Then, the readings of the forces and displacement in the test bed were zeroed and following on from that the contact joint was loaded, thus exciting harmonic runs with amplitude p_a . The force applied on the investigated contact joint of the specimens was directly measured with extensometers glued on the specially designed and shaped sample 2, and the relative contact displacement $\delta(t)$ of samples 1 and 2 with an inductive, non-touch displacement sensor 3, type Tr-20 manufactured by HBM. Signals were recorded on a computer system equipped with S&H system and 16 channel transducer A/D of DAS 1800 type, manufactured by Keithley. "TESTPOINT" software, manufactured by CEC, was used to service the measuring stand. The displacement time runs as well as the applied excitations were recorded with a constant time step and the number of measuring steps, equal to all the experiments, amounted to 32768. The number of load cycles in each trial was 128. The results of the experimental research were saved as ASCII files. Files marked, for graphic presentation of runs and

results of experiments and their appropriate processing, were exported to EXCEL spreadsheet application.

3. Results of experiments

The experiments were conducted on samples whose contact area was greased with a thin layer of LT-43 grease. The recorded fragments of the time runs of pressure and contact displacement, given a mean pressure of $p_o = 0,5$ MPa, amplitude of $p_a = 0,4$ MPa and the frequency of the exciting force $\omega = 1$ 1/s are shown in Fig. 2a and 2b.

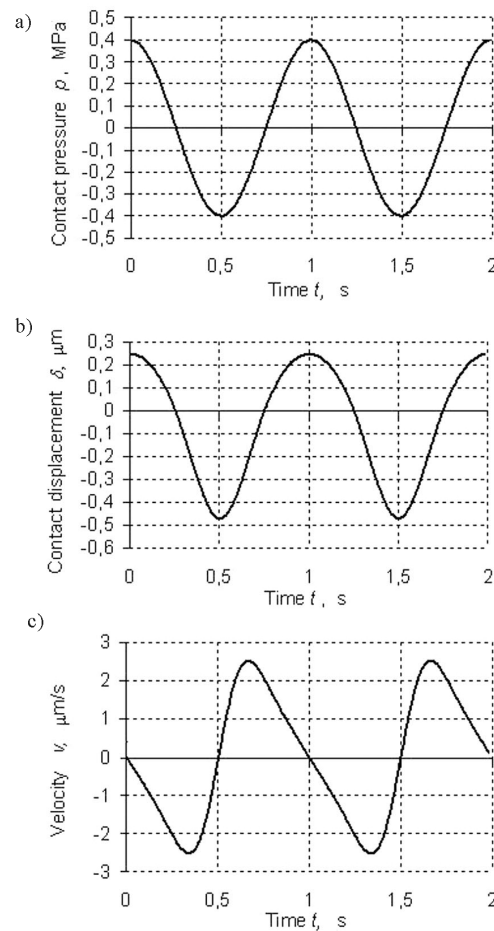


Fig. 2. Time runs of pressures p (a), contact displacement δ (b) and displacement velocity v (c)

The time runs of contact displacement are asymmetrical to the static state of equilibrium. After differentiating these runs, time velocity runs $v(t)$ were obtained. They can be seen in Fig. 2c.

On the basis of the results obtained in the experiments a characteristic showing dependence of contact displacement δ on contact pressure p was determined. The characteristic is shown in Fig. 3. Given the established working conditions, under load and relief of the contact joint, these characteristics run along various lines and create a closed hysteresis loop. The area inside the loop defines the energy dissipated in one, closed load and relief cycle. In order to determine this area, the load curve p_{load} , the relief curve p_{unload} and the centre line p_{centre} located between them were described with a 4th degree polynomial:

$$p = a_0 + a_1\delta + a_2\delta^2 + a_3\delta^3 + a_4\delta^4 \quad (1)$$

where: a_0 - a_4 are constant parameters (Table 2).

Table 2. The values of parameters for the hysteresis loop shown in Fig. 3

Contact pressure	Constant parameters				
	a_0	a_1	a_2	a_3	a_4
p_{load}	0.01541	1.33235	1.49154	2.28094	1.57210
p_{centre}	0	1,32596	1,59811	2,92127	2,87416
p_{unload}	-0.01541	1.31957	1.70468	3.56159	4.17622

The changes in displacement pace of this contact joint depending on the values of contact displacement are presented in the phase portrait (Fig. 4).

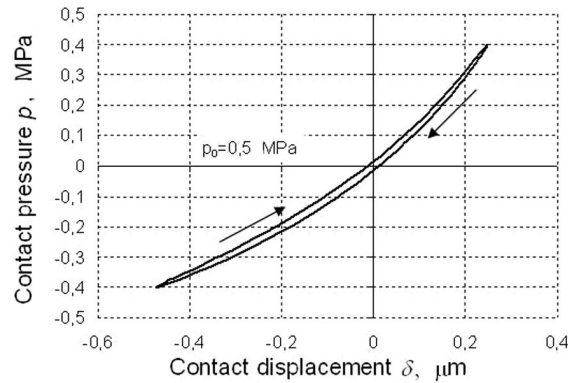


Fig. 3. Dynamic hysteresis loop obtained for the contact joint lubricated with a thin layer of Lt43 grease

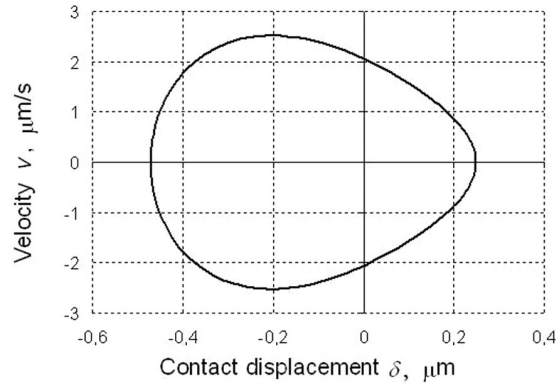


Fig. 4. Phase portrait of the investigated contact.

4. Contact stiffness and damping characteristics

Until now joints between various elements have been substituted in calculations with massless discrete linear spring-damping nodes which can be described with two coefficients which define dynamic stiffness and damping. Real joints in multi-mass systems are usually substituted with massless spring-damping nodes, which meet the criteria set by Kelvin-Voight (Fig. 5a). In this kind of a model, a stable hysteresis loop (at harmonic load) has the shape of ellipse ABCD (Fig. 5b).

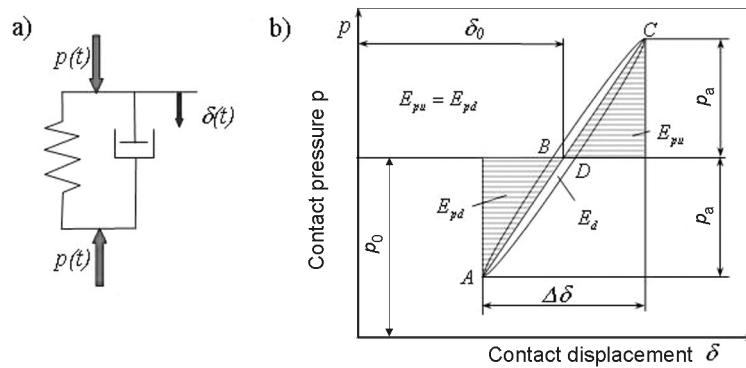


Fig. 5. Scheme (a) and mechanical characteristic for Kelvin-Voight model (b)

In a contact joint total instantaneous contact pressures p_c are the sum of static pressure p_o and dynamic pressure p , which lead to static δ_o and dynamic contact displacement δ . In order to prevent a separation of the surface of the

contact, the amplitude of contact pressure p_a should not exceed static pressure values p_o . Dynamic contact displacement is symmetrical to the static state of equilibrium (Fig. 5b). The values of energy of spring strain during load and relief procedure are equal to each other and they amount to $E_{pd} = E_{pu}$.

In Kelvin-Voight model, the dynamic static stiffness is a constant value which can be given by formula:

$$k_d^{K-V} = \frac{2p_a}{\Delta\delta} = const. \quad (2)$$

The dissipation of vibration energy in Kelvin-Voight model for one vibration cycle (Fig. 5b) is defined by a coefficient of vibration energy ψ_{KV} which can be described as:

$$\psi_{KV} = \frac{E_d}{E_{pu}} \quad (3)$$

where: E_d – is the energy dissipated in one cycle of dynamic load and which is determined by the area of hysteresis loop shaped as ellipse, E_{pu} – is the energy of spring strain which corresponds to maximum amplitude of deflection from the state of equilibrium defined by pressures p_o .

The dynamic hysteresis loops determined during experimental research for a real contact are very different from the shape of ellipse (Fig. 5). Normal characteristics of contacts show asymmetry of displacement from the static state of equilibrium δ_0 defined by pressures p_o . The values of spring energy E_{pu}^n and E_{pd}^n (Fig. 6b) corresponding to maximum deflection from the state of equilibrium are in this case different.

In practice, in calculations of such contact joints, Kelvin-Voight model is also used. On the basis of non-linear characteristics obtained in experiments, equivalent values of contact stiffness and damping are determined. In the range of small amplitudes of dynamic load, the equivalent contact stiffness is determined as the tangent of the inclination angle of the tangent line to AOC line, at point O (Fig. 7):

$$k_d^{\tan} = \text{tg}(a_2) = \left(\frac{dp}{d\delta} \right)_{p=p_0} \quad (4)$$

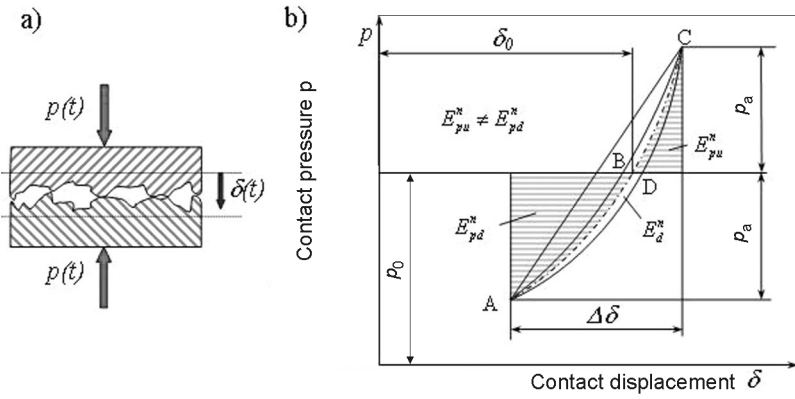


Fig. 6. Scheme showing a contact between flat, machined surfaces (a) and its mechanical characteristic (b)

At higher amplitudes of dynamic load, the equivalent contact stiffness k_d^{sec} can be determined as the tangent of the inclination angle of the secant AC to the axis δ (Fig. 7):

$$k_d^{sec} = \text{tg}(a_1) = \frac{2p_a}{\Delta\delta} \tag{5}$$

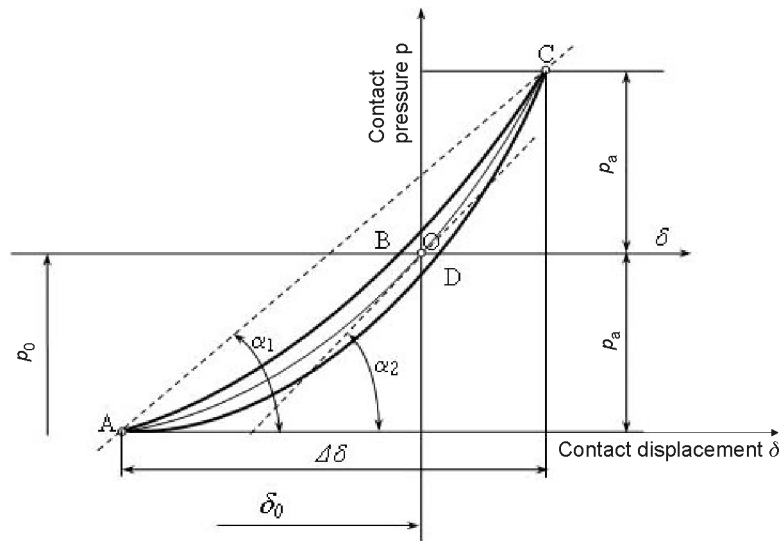


Fig. 7. A diagram of dynamic hysteresis loop determined on the basis of experimental research of the real contact joint

The equivalent values of contact stiffness determined from formulae (4) and (5) are treated as constant values and they do not take into account their changes in the whole range of dynamic load ($\pm p_d$) (Fig. 7). From the course of the line AOC it can be seen that the contact stiffness k_d^s is a changeable variable, which depends on the current dynamic displacement values δ . At points A and C (Fig. 7) it can be much different from the values determined at point O. In order to increase the precision of calculations, dynamic contact stiffness can be given by the following polynomial:

$$k_d^s = \frac{P_{srod}}{\delta} = a_1 + a_2 \cdot \delta + a_3 \cdot \delta^2 + a_4 \cdot \delta^3 \quad (6)$$

The values of dissipation energy of vibrations at the real contact and in the investigated non-linear model should also be equal.

In order to achieve this, it is suggested that the relative coefficient of energy dissipation for the non-linear model of a contact joint should be determined from the following formula:

$$\psi = \frac{2E_d^n}{E_{pu}^n + E_{pd}^n} \quad (7)$$

where: E_d^n – the energy dissipated in one dynamic load cycle and it is determined by the area of hysteresis loop (Fig. 6b), E_{pd}^n, E_{pu}^n – the energy of spring strain (Fig. 6b) for a contact joint with a non-linear characteristics.

5. A model of a contact joint subjected to normal harmonic load

For Kelvin-Voight model, dynamic pressure $p(t)$ at the contact can be given by:

$$p(t) = k_d^{K-V} \cdot \delta(t) + h \cdot v(t) \quad (8)$$

where: $\delta(t)$ – is the normal contact displacement, μm , $v(t)$ – the speed of contact's displacement [$\mu\text{m/s}$], k_d^{K-V} – the constant normal stiffness, $\text{MPa}/\mu\text{m}$, h – the damping coefficient, $\text{MPa s}/\mu\text{m}$.

After applying dynamic load with a harmonic course $p(t)$, the amplitude p_a and the frequency ω , to the contact joint we get, according to formula:

$$p(t) = p_a \cdot \sin(\omega \cdot t) \quad (9)$$

stable time runs of contact displacement, which are described by formula:

$$\delta(t) = K \cdot \sin(\omega \cdot t - \phi) \quad (10)$$

where:

$$K = \frac{p_a}{\sqrt{(k_d^{K-V})^2 + (h \cdot \omega)^2}} \quad (11)$$

$$\phi = \text{arctg} \left(\frac{\omega \cdot h}{k_d^{K-V}} \right) \quad (12)$$

By eliminating from equations (9) and (10) time t we obtain a dependence of dynamic pressures p on the normal contact displacement δ . This dependence is non-linear and in one, closed cycle of load and relief of a contact it takes the shape of an ellipse. The area of this ellipse is the measure of energy dissipation at the contact. Losses of vibration energy is often characterised by the relative coefficient of vibration damping ψ_{KV} (formula 3). In Kelvin-Voight model, the following dependence takes place between coefficients h i ψ_{KV} :

$$h = \frac{k_d^{K-V} \cdot \psi_{KV}}{2 \cdot \pi \cdot \omega} \quad (13)$$

After substituting (13) into (11) and (12), we obtain:

$$K = \frac{p_a}{k_d^{K-V} \sqrt{1 + \left(\frac{\psi_{KV}}{2\pi} \right)^2}} \quad (14)$$

$$\phi = \text{arctg} \left(\frac{\psi_{KV}}{2\pi} \right) \quad (15)$$

In order to determine dynamic characteristics of a non-linear model it is necessary to know the dependence of normal contact stiffness coefficient and the relative coefficient of energy dissipation on contact pressure p . Experimental research has shown that these dependencies are non-linear and that they depend on mean contact pressures p_0 and load amplitude p_a . A diagram showing a model of such a body with variable characteristics of contact stiffness and damping is presented in Fig. 6.

On the basis of conducted experimental research on a contact loaded with mean pressure $p_0 = 0,5-2,5$ MPa and dynamic load with amplitude $p_a = 0,4$ MPa, the dependence of normal contact stiffness coefficient on contact displacement δ given by formula (6), can be expressed as the function of dynamic pressure p :

$$k_d^s = b_1 \cdot p^3 + b_2 \cdot p^2 + b_3 \cdot p + b_4 \quad (16)$$

where: k_d^s – normal contact stiffness expressed, MPa/ μm , p – contact pressure expressed, MPa, b_1 - b_4 – coefficients which depend on mean surface pressure p_0 and pressure amplitude p_a .

The course of changes of normal contact stiffness k_d^s , within the range of amplitude $p_a = \pm 0,4$ MPa for various values of mean contact pressure can be seen in Fig. 8. The relative coefficient of damping Ψ is determined on the basis of the area of hysteresis loop, according to formula (7).

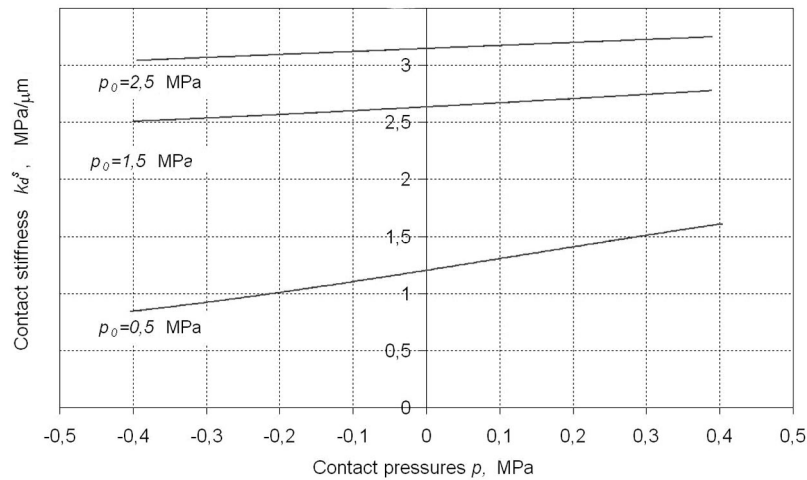


Fig. 8. Dependence of contact stiffness k_d^s on contact pressures

After substituting relation (16) into (13) and (8) ($k_d^{K-V} = k_d^s$) and relation (7) into (13) ($\psi_{KV} = \psi$) we obtained a non-linear model of a contact, which can be given by equation:

$$p(t) = k_d^s \cdot \delta(t) + \frac{k_d^s \cdot \psi}{2\tau \cdot \omega} v(t) \quad (17)$$

In order to compare dynamic characteristics for a model of linear contact and non-linear contact calculations were performed, in which the following data were assumed: $p_0 = 0,5$ MPa, $p_a = 0,4$ MPa, $\omega = 1$ 1/s. For the linear model a constant value of contact stiffness was assumed and this value was defined by formula (4) $k_d^{\tan} = 1.206$ MPa/ μm . It describes normal contact stiffness with dynamic pressures $p = 0$. The relative coefficient of damping was assumed on the basis of experimental research $\Psi = 0.0887$.

The contact characteristics obtained in the calculations were compared with the characteristics obtained in the experiments. They are presented in Fig. 9-12.

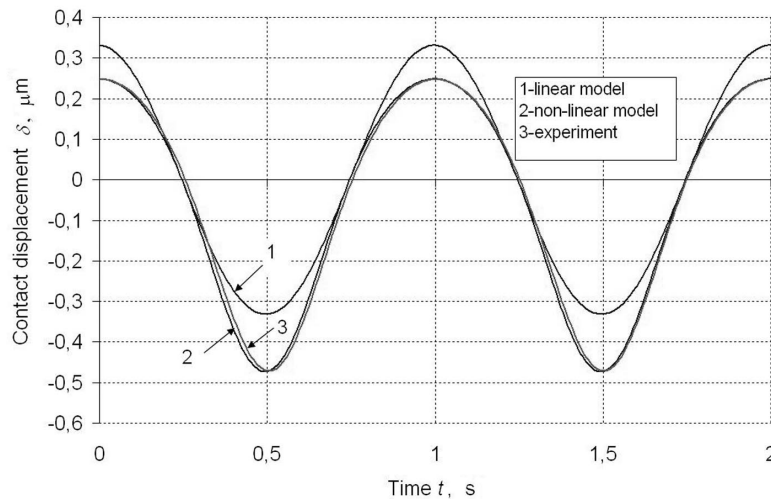


Fig. 9. The course of contact displacements for the linear and non-linear models obtained in the experiments

The course of contact displacements obtained in the calculations for the non-linear model of the contact (line 2, Fig. 9) coincide with the results obtained in the experiments (line 3, Fig. 9). The assumption of a constant contact stiffness in the calculation model (line 1, Fig. 9.) leads to symmetrical runs of contact

displacements. When the contact is loaded, contact displacement is bigger for the linear model than for the non-linear model. When the contact is relieved, displacements are smaller from those obtained for the non-linear model. Extreme values of displacement pace, in load and relief of the contact have the same values (Fig. 10). However, an increase of the pace in a given time, i.e. acceleration, is different in load and relief modes. The non-linear model of the contact more precisely represents time runs of contact displacement than the linear model. This is also evident in the phase graph (Fig. 11).

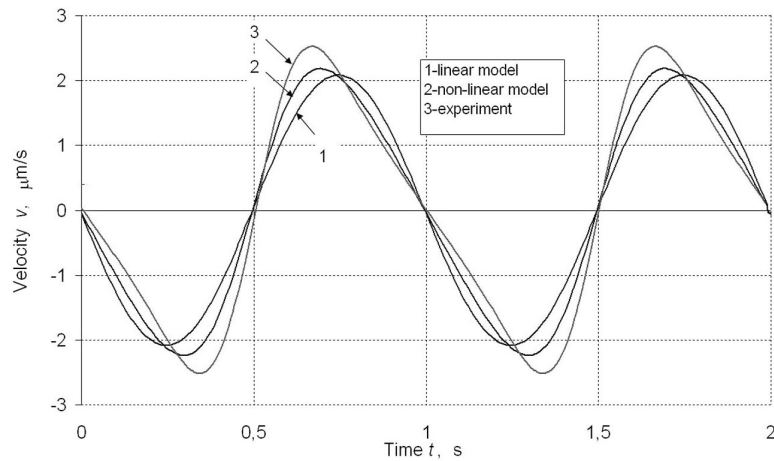


Fig. 10. Velocity courses of the linear and non-linear models and those obtained in the experiments

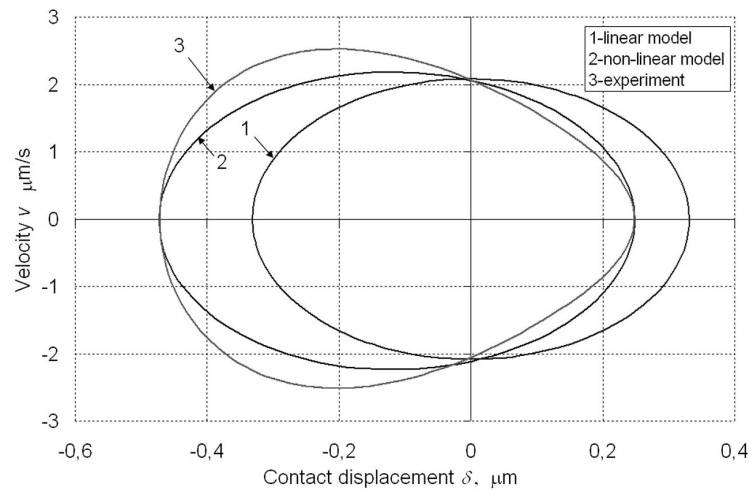


Fig. 11. Phase graphs for the linear and non-linear models and those obtained in the experiments

Hysteresis loops for the non-linear model and those determined in the experiments practically coincide with each other (Fig. 12). This model can well describe, both quantitatively and qualitatively, the real stiffness and damping in the conditions of preset dynamic load.

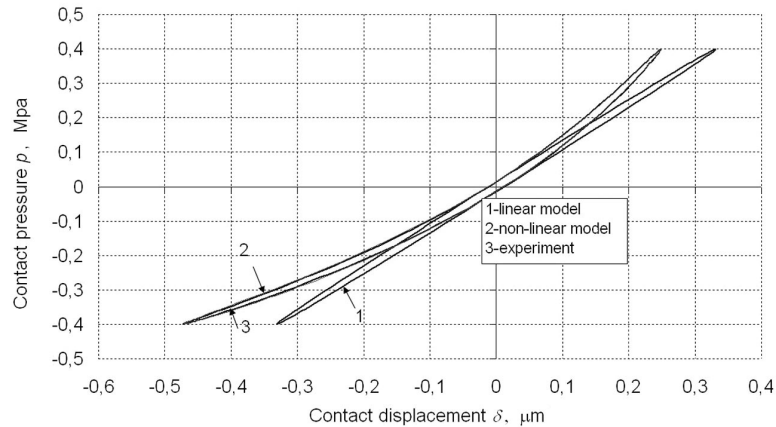


Fig. 12. Hysteresis loops for the linear and non-linear models and those obtained in the experiments

6. Conclusion

On the basis of the conducted experiments it was found that in the range of small contact pressures the dependence of contact deformations on the contact pressures is non-linear. At stable harmonic load conditions, in one closed cycle of load and relief of the contact, these characteristics create closed hysteresis loops. The area within hysteresis loop can be the basis on which it is possible to determine damping in the non-linear model of the contact. When contact stiffness variable (determined on the basis of the experiments) is introduced into the model, the time runs of contact displacement both calculated and obtained in the experiments practically coincide. However, the non-linear model of the contact is not fully equivalent as far as velocities of contact deformations go. The assumption of a constant value of dynamic contact stiffness in the calculations gives, as a result, significant deflections of contact deformation runs and velocity in comparison with the results obtained in the experiments.

References

- [1] Y. Ren, C.F. Beards: Identification of 'effective' linear joints using coupling and joint identification techniques. *ASME Journal of Vibration and Acoustics*, **120** (1998), 331-338.

- [2] W.P. Fu, Y.M. Huang, X.L. Zhang, Q. Guo: Experimental investigation of dynamic normal characteristics of machined joint surfaces. *ASME, Journal of Vibration and Acoustics*, **122** (2000), 393-398.
- [3] K. Marchelek: *Dynamika obrabiarek*. WNT, Warszawa 1991.
- [4] K. Konowalski: Experimental investigations of contact joint under dynamic load. Proc. Fifth Inter. Conf. on Computational Methods in Contact Mechanics, Wessex Institute of Technology, Escuela Superior de Ingenieros, University of Seville, WitPress, Southampton – Boston 2001, 21-30.
- [5] X. Shi, A.A. Policarpou: Measurement and modeling of normal contact stiffness and contact damping at the meso scale. *ASME, Journal of Vibration and Acoustics*, **127**(2005).
- [6] K. Grudziński, K. Konowalski: Badania charakterystyk mechanicznych połączeń stykowych przy obciążeniach dynamicznych. Cz. I. Podstawy badań doświadczalnych i stanowisko badawcze. *Archiwum Technologii Maszyn i Automatyzacji*, **22** (2002)2, 105-114.
- [7] K. Konowalski, K. Grudziński: Badania charakterystyk mechanicznych połączeń stykowych przy obciążeniach dynamicznych. Cz. II. Badania doświadczalne. *Archiwum Technologii Maszyn i Automatyzacji*, **22** (2002)2, 114-127.
- [8] G. Pugliese, S.M.O. Tavares, E. Ciulli, L.A. Ferreira: Rough contacts between actual engineering surfaces, Part II Contact Mechanics. *Wear*, **264**(2008), 1116-1128.
- [9] U. Sellgren, S. Björklund, S. Andersson: A finite element-based model of normal contact between rough surfaces. *Wear*, **254**(2003), 1180-1188.
- [10] ADINA R&C Inc.: Automatic dynamic incremental nonlinear analysis. Theory and modeling guide, Report ARD 02-7, Boston 2002.
- [11] Documentation for ANSYS, Guide to the ANSYS Documentation Contact Technology Guide, Release 11.0.
- [12] P. Wriggers: *Computational Contact Mechanics*. John Wiley&Sons. Ltd., New York 2002.

Received in October 2009